International Journal of Thermophysics, Vol. 21, No. 3, 2000

Binary Diffusion Coefficients of Acetone in Carbon Dioxide at 308.2 and 313.2 K in the Pressure Range from 7.9 to 40 MPa

T. Funazukuri,[1,3] C. Y. Kong,[2] and S. Kagei[2]

Received August 30, 1999

Binary diffusion coefficients of acetone in carbon dioxide were measured by the Taylor dispersion method at 308.2 K and 7.9 to 40 MPa and at 313.2 K and 8.0 to 37 MPa. The D_{12} values obtained from the response curves by the method of fitting in the time domain were more accurate than those obtained by the moment method. At pressures lower than about 8.3 MPa at 308.2 K or 9.1 MPa at 313.2 K, the accuracy in the D_{12} values was found to decrease significantly with decreasing pressure by examining (peak area) $\times u_{a,\mathrm{cal}}$, the values of S_{10}, the fitting error ε, and $u_{a,\mathrm{cal}}/u_{a,\mathrm{exp}}$ as a function of pressure. The D_{12} values at pressures higher than 8.3 MPa at 308.2 K or 9.1 MPa at 313.2 K were well represented with the Schmidt number correlation. The D_{12} data with larger fitting errors ($\varepsilon > 0.01$) showed larger deviations from the values predicted by this correlation.

KEY WORDS: acetone; binary diffusion coefficient; carbon dioxide; Schmidt number correlation; supercritical; Taylor dispersion method.

1. INTRODUCTION

Binary diffusion coefficients D_{12} in supercritical fluids are important for the design of reactors. While a number of measurements [1–38] have been made in supercritical carbon dioxide, they are not sufficient to predict D_{12} values for various solute and supercritical solvent systems over a wide range of temperature and pressure.

[1] Department of Applied Chemistry, Institute of Science and Engineering, Chuo University, 1-13-27 Kasuga, Bunkyo-ku, Tokyo 112-8551, Japan.
[2] Department of Information and Systems, Yokohama National University, 79-5 Tokiwadai, Hodogaya-ku, Yokohama 240-8501, Japan.
[3] To whom correspondence should be addressed.

0195-928X/00/0500-0651$18.00/0

Most of the D_{12} measurements, excluding some studies [1–3, 7–9, 13, 31, 36, 38], were made by the Taylor dispersion method. Although this method was claimed to be moderately accurate (accuracy of ca. 1% by Wakeham et al. [39]), Levelt Sengers et al. [27] pointed out that it was not adequate to employ this method for measurements in the near-critical region. They evaluated the reliability with the skewness obtained from the third moment of the response curve.

Some studies [12, 16, 18, 21, 26, 32, 33, 35, 40] employed the curve-fitting method in the Taylor dispersion, instead of the moment method commonly used. However, the accuracy or reliability in the D_{12} data measured in the Taylor dispersion with the moment method has not been sufficiently evaluated in most studies. Moreover, the moment method leads to erroneous D_{12} values and does not give reliable information when the response peak is distorted or tailing [41]. In other words, the pressure effect on the accuracy of the D_{12} values should be examined because the distortion varies with pressure. The curve-fitting method, however, can be used to examine the reproducibility of the response curves for the D_{12} values determined. In this study, we measure the D_{12} of acetone in carbon dioxide over a wide pressure range by the Taylor dispersion method and examine the accuracy of the D_{12} values in terms of (a) detector linearity in terms of the relationship between the injected amount of acetone and the product of peak area and the velocity u_a, (b) the value of S_{10}, defined as the ratio of the rear half-peak width to the frontal value at 10% peak height, (c) the fitting error, (d) the ratio of the velocity obtained by curve fitting to that measured experimentally, and (e) the effect of the wavelength on the D_{12} values. By examining these effects, the relationship between the reliability in D_{12} data and pressure is more clearly understood. The prediction of D_{12} values is also presented.

2. THEORY

When a tracer species is loaded as a delta shot to a fully developed laminar flow moving in a circular cross-sectional tubing, the tracer concentration is described in Eq. (1), from Taylor [42] and Aris [43]:

$$D_{12}\frac{1}{r}\frac{\partial}{\partial r}\left(r\frac{\partial c}{\partial r}\right)+D_{12}\frac{\partial^2 c}{\partial z^2}=\frac{\partial c}{\partial t}+2u_a\left(1-\frac{r^2}{R^2}\right)\frac{\partial c}{\partial z} \tag{1}$$

where D_{12} is the binary diffusion coefficient of the tracer species, R is the tubing radius, u_a is the average velocity, t is time, and r and z are radial and axial distances, respectively. The initial and boundary conditions are

$$c = \frac{m}{\pi R^2}\delta(z) \qquad \text{at} \quad t = 0 \tag{2}$$

$$\frac{\partial c}{\partial r} = 0 \qquad \text{at} \quad r = 0 \qquad \text{and} \qquad r = R \tag{3}$$

$$c = 0 \qquad \text{at} \quad z = \pm\infty \tag{4}$$

where m is the injected amount of the tracer species. By defining the average concentration per cross-sectional area of tubing given by

$$C = \frac{2}{R^2}\int_0^R cr\, dr \tag{5}$$

Eq. (1) can approximately reduce to Eq. (6):

$$K\frac{\partial^2 C_a}{\partial z^2} - u_a\frac{\partial C_a}{\partial z} = \frac{\partial C_a}{\partial t} \tag{6}$$

where

$$K = D_{12} + \frac{u_a^2 R^2}{48 D_{12}} \tag{7}$$

and C_a is the average concentration per cross-sectional area of tubing which satisfies Eq. (6). Note that C_a is not equal to C; the validity of the approximation of Eq. (6) is examined later. The initial and boundary conditions lead to

$$C_a = \frac{m}{\pi R^2}\delta(z) \qquad \text{at} \quad t = 0 \tag{8}$$

and

$$C_a = 0 \qquad \text{at} \quad z = \pm\infty \tag{9}$$

The solution of Eqs. (6)–(9) is given by Eq. (10):

$$C_a = \frac{m}{\pi R^2 (4\pi K t)^{1/2}} \exp\left[-\frac{(z - u_a t)^2}{4Kt}\right] \tag{10}$$

In this study the D_{12} value is obtained by the method of curve fitting in the time domain (FTD) so that the root-mean-square error ε defined by Eq. (11) is minimized:

$$\varepsilon = \left(\frac{\int_{t_1}^{t_2} (C_{a,\,\mathrm{exp}}(t) - C_{a,\,\mathrm{cal}}(t))^2 \, dt}{\int_{t_1}^{t_2} (C_{a,\,\mathrm{exp}}(t))^2 \, dt} \right)^{1/2} \tag{11}$$

where a fitting period between t_1 and t_2 was chosen so that the measured response curve at higher than 10% peak height is compared with that calculated.

3. EXPERIMENT

A schematic diagram of the experimental apparatus is shown in Fig. 1. The experimental apparatus consists of a syringe pump (Model 100DX, ISCO), a tube for the calming section (0.817-mm I.D. $\times$ 5 m long), a sample injector (Reodyne 7520), a stainless-steel diffusion column (0.817 mm $\times$ 35.00 m, coiled diameter of 250 mm), a multi-UV detector (Multi 320; JASCO, Japan), a back pressure regulator (Model 880-81; JASCO), and a temperature-controlled water bath.

Carbon dioxide (analyzed, its purity higher than 99.9950%, water $<$ 40 ppm; Showa Tansan Co., Japan) was filled into the pump cylinder, whose temperature was maintained at the same value as that of the diffusion column by using the constant-temperature water. The carbon dioxide was fed by the syringe pump at a flow rate from 130 to 265 $\mu l \cdot \mathrm{min}^{-1}$ to the diffusion column via the tubing for calming and the injector. The CO_2 flow velocity was measured by a soap-bubble flow meter after reduction to atmospheric pressure and was also estimated from the measured response curve. The diameter of the diffusion column was 0.817 ± 0.001 mm, obtained from a mean of the diameters of the two ends, as measured by an

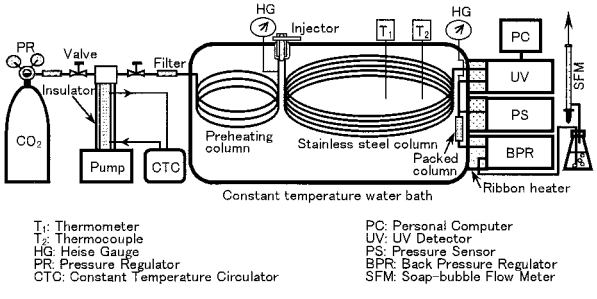

Fig. 1. Schematic diagram of the experimental apparatus.

X-ray microanalyzer (Model JXA; JEOL, Japan). The tubing for calming, the injector, and the diffusion column were immersed to almost the same level in the water bath, while the diffusion column was placed horizontally.

A tracer species of liquid acetone (special grade; Junsei Co., Japan) was loaded via the injector to the diffusion column. The amount of the tracer was approximately 0.5 μl. The time change of the tracer concentration as a response signal was obtained at the exit of the diffusion column with the UV detector, by scanning over wavelengths from 195 to 350 nm. The absorbance data of the responses were recorded with a computer for wavelengths from 195 to 350 nm at increments of 5 nm, corresponding to time intervals of 0.4 to 1.6 s. The temperature of the diffusion column was measured with a calibrated thermometer placed in the vicinity of the column. The temperature fluctuation was less than ± 0.01 K.

The pressure of the system was regulated by the back pressure controller, which is capable of controlling the pressure with a high-frequency open–shut valve operated electromagnetically. A stainless-steel tube packed with fine powder was placed upstream at this pressure controller to further stabilize the pressure. The pressure of the system was measured with the Heise gauge placed just upstream at the injector and with a pressure sensor (CAP-BP01; JEOL) placed just upstream at the packed column. The pressure sensor was calibrated with the two Heise gauges (with ranges up to 10 and 50 MPa). The pressure drop for the diffusion column was less than 0.01 MPa, and that for the packed column was 2 to 5 MPa. The temperature and pressure of carbon dioxide were nearly constant from the cylinder of the syringe pump to the detector, and the pressurized carbon dioxide in the entire lines was kept under supercritical conditions.

4. RESULTS AND DISCUSSION

4.1. Examination of the Validity of the Approximation by Eq. (6)

As the same for most studies, Eq. (1) can be assumed to reduce to Eq. (6). The validity of this assumption is examined with the data shown in Fig. 4, which is described later. The second-order central moment $C^{(2)}$ for the equation in the z space as derived by Aris [43] is

$$C^{(2)} = \int_{-\infty}^{+\infty} (z - u_a t)^2 \, C \, dz \Big/ \left(\frac{m}{\pi R^2} \right)$$

$$= 2Kt - \frac{128 u_a^2 R^4}{D_{12}^2} \sum_{n=1}^{\infty} \frac{1 - \exp(-\lambda_n^2 D_{12} t / R^2)}{\lambda_n^8} \tag{12}$$

where λ_n is the nth root for the first-order Bessel function given by

$$J_1(\lambda_n) = 0 \tag{13}$$

The second-order central moment of C_a is

$$C_a^{(2)} = \int_{-\infty}^{+\infty} (z - u_a t)^2 \, C_a \, dz \Big/ \left(\frac{m}{\pi R^2} \right) = 2Kt \tag{14}$$

Since the first term on the right-hand side of Eq. (12) coincides with Eq. (14), the errors for Eqs. (12) and (14) are equal to the second term in Eq. (12). When $D_{12} = 1.723 \times 10^{-8} \, \mathrm{m^2 \cdot s^{-1}}$ and $u_a = 7.333 \times 10^{-3} \, \mathrm{m \cdot s^{-1}}$, $error_1$ obtained for $t = 75$ to 81 min is

$$error_1 = \left| \frac{C^{(2)} - C_a^{(2)}}{C^{(2)}} \right| = 1.43 \times 10^{-4} \text{ to } 1.33 \times 10^{-4} \tag{15}$$

In comparison, the error for the second-order central moment is defined by

$$error_2 = \left| \frac{\int_0^{+\infty} (z - u_a t)^2 \, C_{a,\,\mathrm{exp}} \, dt - \int_0^{+\infty} (z - u_a t)^2 \, C_{a,\,\mathrm{cal}} \, dt}{\int_0^{+\infty} (z - u_a t)^2 \, C_{a,\,\mathrm{exp}} \, dt} \right| \tag{16}$$

The $error_2$ becomes 0.019 in this case. It is found that the order of $error_1$ is 10^{-4} to 10^{-5}, while that of $error_2$ is 10^{-2} to 10^{-3} under the present measurement conditions. Thus, the approximation can be verified because the fitting error is much larger than the approximation error for Eq. (6).

4.2. Pressure Fluctuation

In the near-critical region, the derivative $d\rho/dP$ is large; thus, it is essential to maintain stable laminar flow without pressure fluctuations during the measurements. It is found that the pressure in the column is so stable that the fluctuation is within ± 2 kPa at pressure noise frequencies of about 1 to 3 Hz over the entire pressure range. The relative pressure fluctuation or the relevant density fluctuation decreased with increasing pressure. Levelt Sengers et al. [27] mentioned difficulty in measuring D_{12} by the Taylor dispersion method in the near-critical region. They estimated that their pressure fluctuation was ± 0.01 MPa at 308 K. If the pressure fluctuation is ± 2 kPa at 308.2 K and 7.94 MPa, the density fluctuation is $\pm 1.0 \, \mathrm{kg \cdot m^{-3}}$ for the current study.

4.3. Effect of Secondary Flow Caused by the Coiling Diffusion Tube

As described in previous studies [6, 44], the effect of secondary flow on D_{12} values caused by the coiling diffusion tube is evaluated by the criterion, $DeSc^{1/2} < Q$. When Q is 8, the error is estimated to be 1% [44]. In this study the values of $DeSc^{1/2}$ were always lower than 8. Thus, the effect is negligible.

4.4. Detector Linearity with Respect to Peak Area

Figure 2a shows the values of (peak area) $\times u_{a,\mathrm{cal}}$ vs pressure at 308.2 and 313.2 K in the pressure range from 7.9 to 40 MPa. Since the values are proportional to the tracer amount injected, the values should be constant independent of pressure. As shown, the values are constant at pressures above 20 MPa for both temperatures and decrease slightly with decreasing pressure up to 10 MPa. At pressures lower than 10 MPa, the values drop sharply with decreasing pressure, show minimum values at about 8.8 MPa, and then increase with decreasing pressure. The values for some runs, however, do not decrease in the pressure range even from 8.8 to 10 MPa, and the values show large deviations (5 to 30%) in this region. Note that

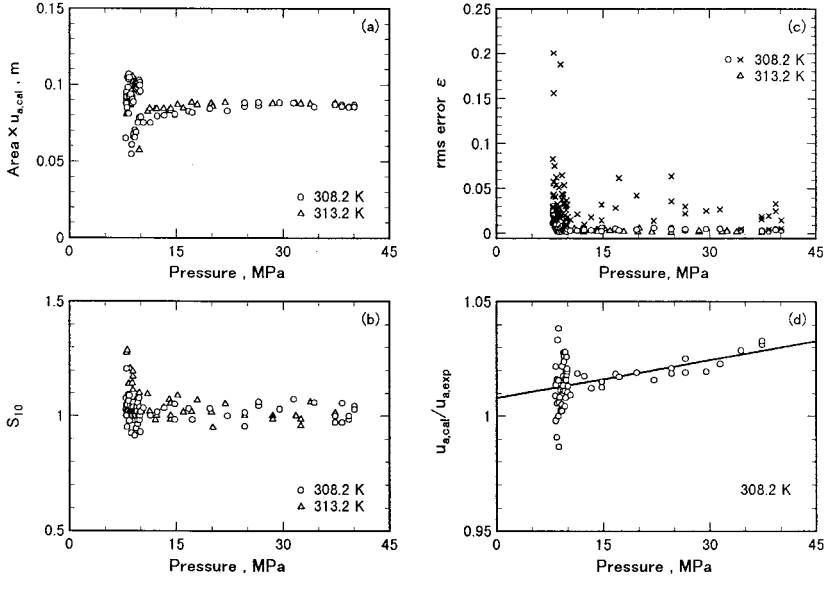

Fig. 2. Effects of pressure on measurement accuracy for the FTD method: (a) peak area $\times u_{a,\mathrm{cal}}$, (b) S_{10}, (c) fitting error ε, together with ε for the moment method at 308.2 K (×), and (d) velocity ratio of $u_{a,\mathrm{cal}}/u_{a,\mathrm{exp}}$, at 308.2 K (○) and 313.2 K (△).

the deviation in the plot of the values of (peak area) $\times u_{a,\,\mathrm{cal}}$ vs pressure was not correlated with the fitting error at pressures lower than 10 MPa.

4.5. Peak Distortion

Figure 2b shows the effect of pressure on the value of S_{10}, defined as the ratio of the latter half-peak width to the frontal value at 10% of the peak height, as used previously [6]. In the region where the initial effect can be eliminated, namely, when a sufficiently long column is employed as in the present study, the response curve is expressed by the Gaussian distribution function. This is almost symmetrical, and the S_{10} value is nearly unity. Note that the response curve is not symmetrical theoretically; see Eq. (10). When the S_{10} value deviates from unity, Lauer et al. [6] claimed that adsorption of the tracer species onto the inside wall of the column might take place. The value is almost unity at pressures higher than 10 MPa at both temperatures, but the values for some data show deviations at pressures lower than 10 MPa. The reason for the deviation is not clear, but this is consistent with the observation by Levelt Sengers et al. [27] as the critical pressure is approached from higher pressures.

4.6. Fitting Error

Figure 2c compares fitting errors ε for the FTD at 308.2 and 313.2 K with those for the moment methods at 308.2 K, at pressures from 7.9 to 40 MPa. The errors for the FTD method are found to be much lower than those for the moment method, while the errors for both methods abruptly increase with decreasing pressure at pressures lower than about 10 MPa. The increases correspond to the deviations for the values of (peak area) $\times$ $u_{a,\,\mathrm{cal}}$ and S_{10}. The maximum fitting error ε for the FTD method was 3.0% at 308.2 K and 8.06 MPa and, correspondingly, 20.1% for the moment method. It is found that at pressures higher than 8.3 MPa at 308.2 K, the average fitting error for the FTD method is 0.52% for 63 data points, while it is 3.19% for the moment method.

4.7. Velocity Deviation

Figure 2d shows the ratio of the velocity obtained by curve fitting to that measured with a soap-bubble flow meter at the very end of the system at atmospheric pressure. It is found that the ratio is slightly larger than unity, by 1.5 to 3%, at pressures higher than 10 MPa. This could be caused by the experimental error and/or the resistance of soap film. However, the values drop sharply with decreasing pressure at lower pressures. This

behavior is consistent with the observations shown in Fig. 2a–c. The distinct anomaly in these values at pressures lower than 10 MPa is caused mainly by the asymmetric response curve. Note that the deviations of the values of (peak area) $\times u_{a,\,\mathrm{cal}}$, S_{10}, fitting error, and $u_{a,\,\mathrm{cal}}/u_{a,\,\mathrm{exp}}$ were found to be largely uncorrelated at pressures lower than 10 MPa. It can be considered that the deviations do not result from experimental error but from the characteristic behavior in the near-critical region.

4.8. Effect of Absorption Wavelength

Figure 3 shows the effects of absorption wavelength on (a) absorbance intensities at maximum peak height of the response curve, (b) the root-mean-square fitting error ε defined by Eq. (11), and (c) determined D_{12}

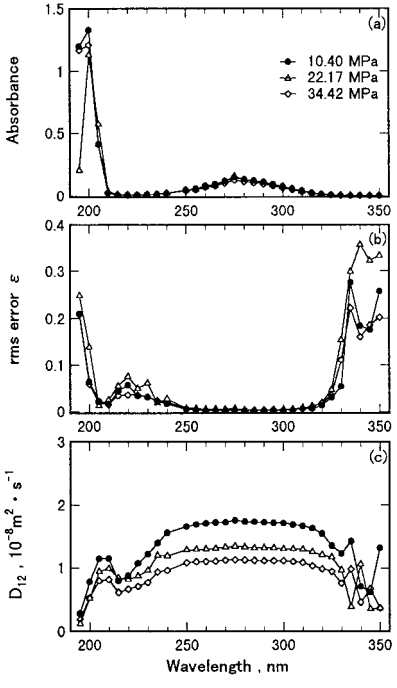

Fig. 3. Effects of wavelength on (a) absorbance spectra at the maximum peak height, (b) fitting error ε defined by Eq. (11), and (c) D_{12}, at 308.2 K and pressures of 10.40 MPa (●), 22.17 MPa (△), and 34.42 MPa (◇) with 0.5 μl acetone injected.

values, at 308.2 K and three pressures, 10.40, 22.17, and 34.42 MPa. The response curves were obtained at wavelengths from 195 to 350 nm at increments of 5 nm for each measurement, and the D_{12} values were determined for each wavelength. It is found that the absorbance intensities show maxima at about 275 nm for the measurements at the three pressures except for too strong intensities at 195 to 210 nm. Correspondingly, the fitting errors showed minimum values at about 250 to 310 nm, and the determined D_{12} values were almost-constant, independent of wavelength from 250 to 310 nm. In this study the D_{12} values were determined from the response curves measured at 265 nm.

4.9. Parameter Sensitivity

Figure 4a shows the response curves calculated by the FTD method for the best fit, and by the moment method, together with that measured experimentally at 308.2 K and 10.40 MPa. Figure 4b shows comparisons of the deviations from the measured absorbance values for both methods for

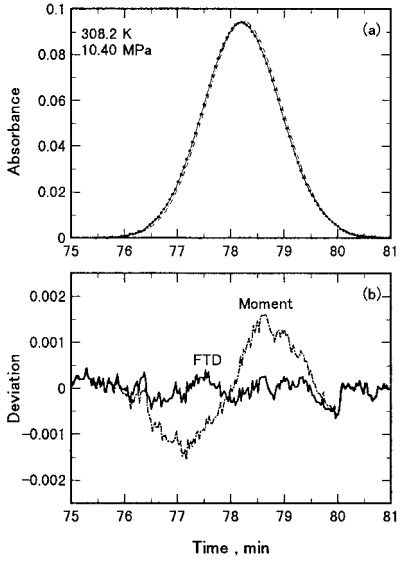

Fig. 4. Comparison between the FTD method and the moment method at 308.2 K and 10.40 MPa; (a) response curves observed experimentally (•) and calculated (——, FTD; – · – · –, moment) and (b) deviations of calculated values from measured results.

the data shown in Fig. 4a. The deviation for the FTD method is found to be quite low over the complete time range of the response curve.

Figure 5 shows the fitting error contour map for the data at 308.2 K and 10.40 MPa shown in Fig. 4. In the FTD method, the two values of D_{12} and u_a are assumed to be adjustable parameters. This figure implies that all data sets of D_{12} and u_a having the same value of fitting error lead to the same accuracy in the value of D_{12} determined. It is found that the D_{12} value is $D_{12} = 1.723 \times 10^{-8}\ \mathrm{m^2 \cdot s^{-1}}$ at the lowest fitting error ε of 0.0033 by the FTD method. Figure 5 shows the effective ranges of velocity u_a from 7.3317×10^{-3} to $7.3335 \times 10^{-3}\ \mathrm{m \cdot s^{-1}}$ if the fitting error is less than 0.01. The values of D_{12} and u_a obtained by the moment method are $1.753 \times 10^{-8}\ \mathrm{m^2 \cdot s^{-1}}$ and $7.3312 \times 10^{-3}\ \mathrm{m \cdot s^{-1}}$, respectively. The corresponding fitting error is 0.015, denoted by the symbol $\times$ in the figure. Thus, the D_{12} value by the moment method deviates from that for the best fit.

4.10. D_{12} Values

Data of D_{12} measured at 308.2 and 313.2 K are listed together with the fitting error ε in Tables I and II. Figure 6 also shows data of D_{12} measured vs pressure at both temperatures in the pressure range from 7.9 to 40 MPa, together with literature D_{12} values at about 308 and 313 K, which were all measured by the Taylor dispersion method. It is found that the D_{12} values decrease simply with increasing pressure. The data of Nishiumi et al. [34] at 314.3 K shift toward lower D_{12} values, and those of Dahmen et al. [14]

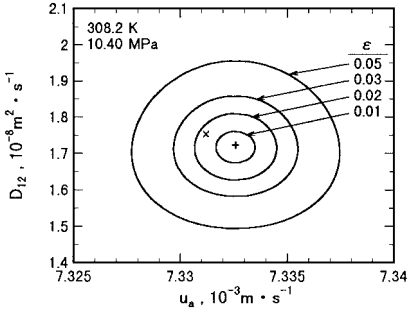

Fig. 5. Error contour map for D_{12} vs interstitial velocity u_a at 308.2 K and 10.40 MPa: +, best fit for the FTD method with $\varepsilon = 0.0033$, $u_a = 7.3325 \times 10^{-3}\ \mathrm{m \cdot s^{-1}}$, and $D_{12} = 1.723 \times 10^{-8}\ \mathrm{m^2 \cdot s^{-1}}$; $\times$, moment method with $\varepsilon = 0.015$, $u_a = 7.3312 \times 10^{-3}\ \mathrm{m \cdot s^{-1}}$, and $D_{12} = 1.753 \times 10^{-8}\ \mathrm{m^2 \cdot s^{-1}}$.

Table I. Measured Binary Diffusion Coefficients of Acetone in Supercritical Carbon Dioxide at 308.2 K

Pressure (MPa)	D_{12} (10^{-8} m$^2 \cdot$ s^{-1})	Fitting error ε	Pressure (MPa)	D_{12} (10^{-8} m$^2 \cdot$ s^{-1})	Fitting error ε	Pressure (MPa)	D_{12} (10^{-8} m$^2 \cdot$ s^{-1})	Fitting error ε
7.94	3.360	0.0116	9.00	2.130	0.0061	10.40	1.723	0.0033
7.97	3.106	0.0249	9.00	1.986	0.0052	11.38	1.631	0.0033
7.97	3.145	0.0226	9.01	1.963	0.0063	12.36	1.581	0.0040
8.05	2.653	0.0249	9.19	1.865	0.0149	13.34	1.553	0.0038
8.06	2.969	0.0304	9.21	2.039	0.0080	14.81	1.484	0.0027
8.06	2.750	0.0205	9.22	2.024	0.0022	14.81	1.465	0.0064
8.07	2.979	0.0192	9.40	1.954	0.0035	16.77	1.397	0.0056
8.08	2.890	0.0147	9.40	1.988	0.0091	17.26	1.427	0.0037
8.17	2.780	0.0130	9.41	2.036	0.0036	19.71	1.358	0.0047
8.17	2.916	0.0102	9.42	2.106	0.0034	22.17	1.309	0.0066
8.26	2.964	0.0074	9.50	2.031	0.0028	24.62	1.245	0.0064
8.26	2.676	0.0104	9.51	1.933	0.0027	24.62	1.261	0.0049
8.33	2.707	0.0091	9.60	1.872	0.0047	26.58	1.204	0.0049
8.36	2.513	0.0064	9.60	1.935	0.0021	26.58	1.231	0.0035
8.36	2.428	0.0053	9.61	2.044	0.0071	29.52	1.171	0.0049
8.44	2.399	0.0100	9.70	1.912	0.0037	31.48	1.133	0.0053
8.44	2.816	0.0048	9.74	1.883	0.0033	34.42	1.110	0.0034
8.53	2.461	0.0029	9.78	1.989	0.0060	37.37	1.096	0.0035
8.62	2.218	0.0041	9.81	1.838	0.0031	37.37	1.099	0.0026
8.70	2.294	0.0206	9.83	1.896	0.0067	38.35	1.045	0.0033
8.72	2.290	0.0051	9.88	1.837	0.0070	38.35	1.068	0.0030
8.73	2.127	0.0037	9.91	1.839	0.0025	39.33	1.068	0.0052
8.79	1.964	0.0067	9.91	1.882	0.0023	39.33	1.075	0.0040
8.82	2.289	0.0100	9.96	1.925	0.0135	40.11	1.065	0.0036
8.90	2.201	0.0015	10.03	1.769	0.0047	40.11	1.060	0.0037

Table II. Measured Binary Diffusion Coefficients of Acetone in Supercritical Carbon Dioxide at 313.2 K

Pressure (MPa)	D_{12} (10^{-8} m$^2 \cdot$ s^{-1})	Fitting error ε	Pressure (MPa)	D_{12} (10^{-8} m$^2 \cdot$ s^{-1})	Fitting error ε	Pressure (MPa)	D_{12} (10^{-8} m$^2 \cdot$ s^{-1})	Fitting error ε
8.04	2.857	0.0225	9.44	2.337	0.0092	15.99	1.602	0.0031
8.14	3.728	0.0552	9.44	2.670	0.0052	17.16	1.562	0.0033
8.34	2.985	0.0218	9.51	2.542	0.0062	17.95	1.488	0.0024
8.53	3.956	0.0172	9.81	2.213	0.0101	19.91	1.458	0.0016
8.53	3.051	0.0148	10.01	2.121	0.0031	20.11	1.488	0.0063
8.83	2.647	0.0104	10.13	2.121	0.0031	21.87	1.424	0.0018
8.83	2.684	0.0216	10.99	1.933	0.0057	24.62	1.349	0.0012
8.93	2.930	0.0165	11.28	2.038	0.0031	28.54	1.268	0.0020
8.93	3.042	0.0262	12.06	1.780	0.0055	28.54	1.266	0.0031
8.93	2.677	0.0182	12.26	1.932	0.0019	31.78	1.184	0.0020
9.04	2.710	0.0113	13.24	1.811	0.0031	32.46	1.216	0.0033
9.14	2.735	0.0050	14.03	1.703	0.0043	32.46	1.201	0.0023
9.24	2.630	0.0081	14.22	1.609	0.0022	33.84	1.188	0.0020
9.32	2.449	0.0081	14.22	1.676	0.0026	37.37	1.147	0.0014
9.33	2.589	0.0073	14.22	1.679	0.0039			
9.42	2.813	0.0032	15.20	1.650	0.0055			

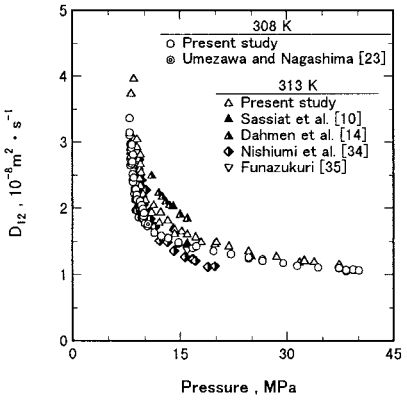

Fig. 6. Binary diffusion coefficients obtained by the FTD method vs pressure at 308.2 K (○) and 313.2 K (△), together with literature data at about 308 and 313 K.

at 313.2 K are higher. The data of Sassiat et al. [10] at 313.2 K at lower pressures are consistent with the present data.

4.11. Schmidt Number Correlation

Funazukuri and Wakao [26] proposed the Schmidt number correlation for predicting binary diffusion coefficients as well as self-diffusion coefficients from low to high pressure regions as follows:

$$Sc^+ = \frac{Sc}{Sc^*} = 1 + \exp\left[\sum_{i=0}^{5} a_i \left(\frac{v_0}{v}\right)^i\right] \tag{17}$$

where

$$Sc^* = \frac{5}{6}\left[\frac{\sigma_1 + \sigma_2}{2\sigma_2}\right]^2 \left[\frac{2M_1}{M_1 + M_2}\right]^{1/2} \qquad \text{for binary diffusion}$$

and

$$Sc^* = \tfrac{5}{6} \qquad \text{for self-diffusion}$$

The coefficients a_i are listed in Table III, and Sc and Sc^* are Schmidt numbers at high pressure and at atmospheric pressure at the same temperature, respectively; v is the molar volume of the solvent; v_0 is the hard-sphere closest-packed volume of solvent molecules; and σ_1 and σ_2 are hard-sphere

Table III. Correlation[a] of Schmidt Number with Solvent Molar Volume [26]

i	a_i
0	-4.92519817
1	5.45529385×10^1
2	-2.45231443×10^2
3	6.07893924×10^2
4	-7.08884016×10^2
5	3.29611433×10^2

[a] $Sc^+ = 1 + \exp[\sum_{i=0}^{5} a_i (v_0/v)^i]$, where $v_0 = N\sigma^3/\sqrt{2}$, N is Avogadro's number, and σ is the effective hard-sphere diameter.

diameters for the solute and solvent, respectively. The σ_2 value is obtained from the v_0 correlation with temperature [21]. When the σ_1 value is not available, the following assumption is made:

$$\frac{\sigma_1}{\sigma_2} = \frac{\sigma_{\text{vw, 1}}}{\sigma_{\text{vw, 2}}} \tag{18}$$

where $\sigma_{\text{vw, 1}}$ and $\sigma_{\text{vw, 2}}$ are van der Waals diameters of solute and solvent molecules, respectively, obtained from the method of Bondi [45].

Figure 7 shows the plot for the Schmidt number correlation for the D_{12} data measured in this study. Note that the Schmidt number correlation does not have any specific adjustable parameters for the solute. It is found that the present D_{12} data having low fitting errors ($\varepsilon < 0.01$ for open symbols) are well represented by the correlation at both temperatures in the wide pressure range (from 8.3 to 40 MPa at 308.2 K and from 9.1 to 37 MPa at 313.2 K), while the data having higher fitting errors ($\varepsilon > 0.01$ for filled symbols) show larger deviations from the correlation. Higashi et al. [36] pointed out that this correlation provides a good representation of their experimental values for D_{12} of naphthalene in CO_2. Figure 8 compares literature data with the correlation. The deviations of most literature data are larger than the present data. The data of Sassiat et al. [10] and Umezawa and Nagashima [23] at lower pressures are roughly consistent with those from the correlation.

5. CONCLUSIONS

Binary diffusion coefficients of acetone in carbon dioxide were measured at 308.2 and 313.2 K in the pressure range from 7.9 to 40 MPa

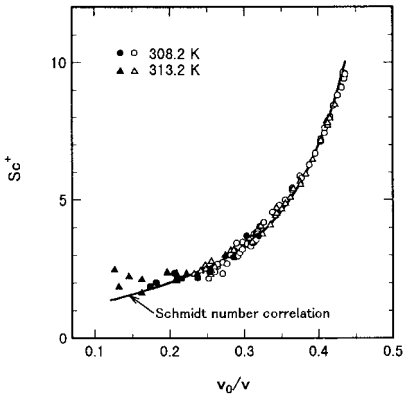

Fig. 7. Plot for the Schmidt number correlation for the D_{12} values measured at 308.2 K and at 313.2 K: (○) $\varepsilon < 0.01$ and (●) $\varepsilon > 0.01$ at 308.2 K; (△) $\varepsilon < 0.01$ and (▲) $\varepsilon > 0.01$ at 313.2 K.

by the Taylor dispersion method. The FTD method was more accurate than the moment method to obtain binary diffusion coefficients from the response curves. At pressures lower than 8.3 MPa at 308.2 K and 9.1 MPa at 313.2 K, corresponding to CO_2 densities of 572 $kg \cdot m^{-3}$ at 308.2 K and 510 $kg \cdot m^{-3}$ at 313.2 K, the accuracy in the D_{12} values decrease sharply with decreasing pressure. This observation can be supported by examining (peak area) $\times u_{a,\,cal}$, values of S_{10}, the fitting error, and $u_{a,\,cal}/u_{a,\,exp}$ with

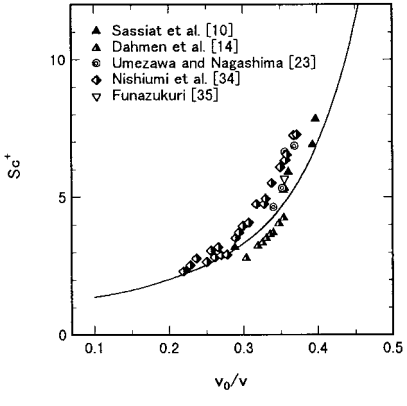

Fig. 8. Comparison of literature data with values predicted by the Schmidt number correlation.

pressure. The D_{12} values having low fitting errors ($\varepsilon < 0.01$, corresponding to pressures higher than 8.3 MPa at 308.2 K or 9.1 MPa at 313.2 K) were well represented by the Schmidt number correlation.

ACKNOWLEDGMENTS

The authors are grateful to the Institute of Science and Engineering of Chuo University for a project research grant and the Ministry of Education of Japan for a research facility grant for graduate school in private universities. The authors also thank Mr. Y. Shimada of the Instrumental Analysis Center of Yokohama National University for measuring the inner diameter of the diffusion tubing with an X-ray microanalyzer.

NOMENCLATURE

c	Tracer concentration
C	Average concentration defined by Eq. (5)
C_a	Average concentration defined by Eq. (6)
$C^{(2)}$	Second-order central moment of C
$C_a^{(2)}$	Second-order central moment of C_a
D_{12}	Binary diffusion coefficient
De	Dean number
M	Molecular weight
m	Injected amount of tracer
P	Pressure
R	Tube radius
r	Radial distance
Sc	Schmidt number
t	Time
u_a	Average velocity
v	Molar volume
v_0	Hard-sphere closest-packed volume
z	Axial distance
ε	Error defined by Eq. (11)
ρ	Density
σ	Hard-sphere diameter

Subscripts

cal	Calculation
exp	Experimental

vw Van der Waals
1 Solute
2 Solvent

REFERENCES

1. M. B. Iomtev and Y. V. Tsekhanskaya, *Russ. J. Phys. Chem.* **38**:485 (1964).
2. Y. V. Tsekhanskaya, *Russ. J. Phys. Chem.* **45**:744 (1971).
3. E. G. Vinkler and V. S. Morozov, *Russ. J. Phys. Chem.* **49**:1405 (1975).
4. I. Swaid and G. M. Schneider, *Ber. Bunsenges. Phys. Chem.* **83**:969 (1979).
5. R. Feist and G. M. Schneider, *Sep. Sci. Technol.* **17**:261 (1982).
6. H. H. Lauer, D. McManigill, and R. D. Board, *Anal. Chem.* **55**:1370 (1983).
7. H. Saad and E. Gulari, *Ber. Bunsenges. Phys. Chem.* **88**:834 (1984).
8. P. G. Debenedetti and R. C. Reid, *AIChE J.* **32**:2034 (1986).
9. G. Knaff and E. U. Schlünder, *Chem. Eng. Process.* **21**:101 (1987).
10. P. R. Sassiat, P. Mourier, M. H. Caude, and R. H. Rosset, *Anal. Chem.* **59**:1164 (1987).
11. T. J. Bruno, *J. Res. Nat. Inst. Stand. Technol.* **94**:105 (1989).
12. T. Funazukuri, S. Hachisu, and N. Wakao, *Anal. Chem.* **61**:118 (1989).
13. D. M. Lamb, S. T. Adamy, K. W. Woo, and J. Jonas, *J. Phys. Chem.* **93**:5002 (1989).
14. N. Dahmen, A. Kordikowski, and G. M. Schneider, *J. Chromatogr.* **505**:169 (1990).
15. N. Dahmen, A. Dülberg, and G. M. Schneider, *Ber. Bunsenges. Phys. Chem.* **94**:384 (1990)/Erratum, **94**:710 (1990).
16. C. Erkey, H. Gadalla, and A. Akgerman, *J. Supercrit. Fluids* **3**:180 (1990).
17. T. J. Bruno, *Supercritical Fluid Technology: Reviews in Modern Theory and Applications*, T. J. Bruno and J. F. Ely, eds. (CRC Press, New York, 1991), pp. 293–324.
18. T. Funazukuri, S. Hachisu, and N. Wakao, *Ind. Eng. Chem. Res.* **30**:1323 (1991).
19. K. K. Liong, P. A. Wells, and N. R. Foster, *Ind. Eng. Chem. Res.* **30**:1329 (1991).
20. S. V. Olesik and J. L. Woodruff, *Anal. Chem.* **63**:670 (1991).
21. T. Funazukuri, Y. Ishiwata, and N. Wakao, *AIChE J.* **38**:1761 (1992).
22. K. K. Liong, P. A. Wells, and N. R. Foster, *Ind. Eng. Chem. Res.* **31**:390 (1992).
23. S. Umezawa and A. Nagashima, *J. Supercrit. Fluids* **5**:242 (1992).
24. T. Wells, N. R. Foster, and R. P. Chaplin, *Ind. Eng. Chem. Res.* **31**:927 (1992).
25. J. L. Bueno, J. J. Suárez, J. Dizy, and I. Medina, *J. Chem. Eng. Data* **38**:344 (1993).
26. T. Funazukuri and N. Wakao, Preprint of the AIChE fall meeting (New Orleans, 1993).
27. J. M. H. Levelt Sengers, U. K. Deiters, U. Klask, P. Swidersky, and G. M. Schneider, *Int. J. Thermophys.* **14**:893 (1993).
28. V. M. Shenai, B. L. Hamilton, and M. A. Matthews, ACS Symp. Ser. 514, *Supercritical Fluid Engineering Science*, E. Kiran and J. F. Brennecke, eds. (1993), pp. 92–103.
29. J. J. Suárez, J. L. Bueno, and I. Medina, *Chem. Eng. Sci.* **48**:2419 (1993).
30. O. J. Catchpole and M. B. King, *Ind. Eng. Chem. Res.* **33**:1828 (1994).
31. C. C. Lai and C. S. Tan, *Ind. Eng. Chem. Res.* **34**:674 (1995).
32. A. Akgerman, C. Erkey, and M. Orejuela, *Ind. Eng. Chem. Res.* **35**:911 (1996).
33. T. Funazukuri and N. Nishimoto, *Fluid Phase Equil.* **125**:235 (1996).
34. H. Nishiumi, M. Fujita, and K. Agou, *Fluid Phase Equil.* **117**:356 (1996).
35. T. Funazukuri, *J. Chem. Eng. Japan* **29**:191 (1996).
36. H. Higashi, Y. Iwai, Y. Takahashi, H. Uchida, and Y. Arai, *Fluid Phase Equil.* **144**:269 (1998).
37. C. M. Silva and E. A. Macedo, *Ind. Eng. Chem. Res.* **37**:1490 (1998).
38. D. Q. Tuan, M. E. Yener, J. A. Zollweg, P. Harriott, and S. S. H. Rizvi, *Ind. Eng. Chem. Res.* **38**:554 (1999).

39. W. A. Wakeham, A. Nagashima, and J. V. Sengers, *Measurement of the Transport Properties of Fluid* (Blackwell Scientific, Oxford, 1991), p. 233.
40. T. Funazukuri, N. Nishimoto, and N. Wakao, *J. Chem. Eng. Data* **39**:911 (1994).
41. N. Wakao and S. Kaguei, *Heat and Mass Transfer in Packed Beds* (Gordon and Breach, New York, 1982), p. 18.
42. G. Taylor, *Proc. Roy. Soc. London* **A219**:186 (1953).
43. R. Aris, *Proc. Roy. Soc. London* **A235**:67 (1956).
44. A. Alizadeh, C. A. Nieto de Castro, and W. A. Wakeham, *Int. J. Thermophys.* **1**:243 (1980).
45. A. Bondi, *J. Phys. Chem.* **68**:441 (1964).